Pergamon

Cement and Concrete Research 32 (2002) 557–563

CEMENT AND CONCRETE RESEARCH

Hardening process of cement-based materials monitored by the instrumented penetration test
Part 1: Neat cement paste and mortar

Donggy Sohn[a], D. Lynn Johnson[b,*]

[a]*Hankook Lock Industry Co. Ltd., Seoul, 136-113, South Korea*
[b]*Department of Materials Science and Engineering, Northwestern University, Evanston, IL 60208-3108, USA*

Received 13 March 1999; accepted 29 October 2001

Abstract

Little fundamental understanding of hardening of cement-based materials can be derived from the standard tests, such as the Vicat needle (ASTM C191-82) and penetration resistance (ASTM 403) tests. A new instrumented penetration test has been developed which continuously monitors the hardness development during early hydration and enables greater understanding of details of the hardening process. The test was designed to measure hardening in situ under ambient temperature or during microwave heating. Descriptive models of the hardening response to selected processing variables for paste as well as mortar were established using statistical experimental designs. The water/cement (w/c) ratio and temperature significantly influenced hardening, while the effect of the amount of sand on hardening was negligible. Several interactions among processing variables were observed to affect hardening. Rheological as well as chemical effects were observed.

Keywords: Acceleration; Hydration; Kinetics; Microwave processing; Thermal treatment

1. Introduction

It is well known that chemical reactions between cement and water transform cement pastes, mortars and concrete from fluids to rigid bodies. The materials remain workable within a dormant period because further hydration is retarded by hydration products that form around the cement grains early [1]. When these coatings are ruptured by osmotic pressure, hydration is resumed and the setting process takes place [2].

The term *setting* has been used to describe the onset of rigidity in fresh cement paste and concrete [3–5]. The phenomena of setting can be altered by some factors, such as water/cement (w/c) ratio [6], curing temperature [7] and admixtures [8,9]. Concrete, mortar or cement paste, which have higher water content or are cured at lower temperature, tend to set more slowly. The admixture effects on the setting vary significantly due to wide variations in their chemical compositions.

Thermodynamically, the initial set is marked by a rapid temperature rise, which corresponds roughly to the beginning of the main chemical reactions. This temperature rise will reach a maximum rate around the final set. However, the relationships between the chemical and physical manifestations are unclear because of lack of information about hardness development during the hydration process.

Recently, a newly developed instrumented penetration test has been developed which provides a useful tool for monitoring early hardening process of cement-based materials [10,11]. Since the penetration test performs in situ and continuous measurement of the hardness development during hydration, it is able to provide more information regarding the cement hydration process than the conventional tests. The setting times and hardening kinetics of various cement-based materials were successfully measured by this test [10–12].

The objective of this study was to establish the scientific and engineering basis for understanding the hardness development during hydration of cement-based materials by using

* Corresponding author. Tel.: +1-847-491-3584; fax: +1-847-491-7820.

E-mail address: dl-johnson@northwestern.edu (D.L. Johnson).

0008-8846/02/$ – see front matter
PII: S0008-8846(01)00721-9

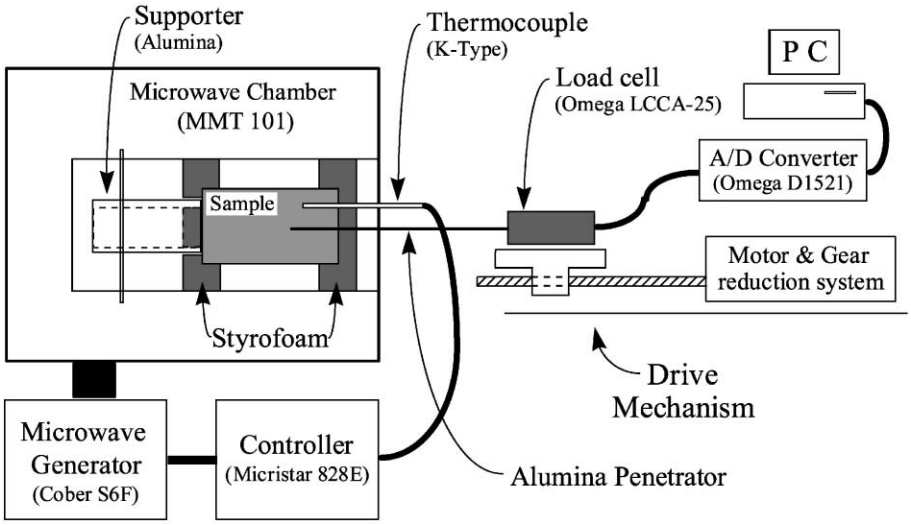

Fig. 1. Schematic diagram of instrumented penetration test and microwave oven.

the instrumented penetration test. Statistical approaches were employed, managing several variables which may affect the hardness development.

2. Experimental procedure

2.1. Apparatus

The in situ hardness development of cement paste or mortar was measured at room temperature and with microwave heating by the instrumented penetration test, shown schematically in Fig. 1. The specimen was placed inside a highly overmoded cylindrical microwave oven (MMT 101, Oak Ridge, TN; $\Phi = 0.75$ m, $L = 1.2$ m) whose power was regulated by the feedback system according to the specimen temperature. A load cell (Omega LCCA-25, Stamford, CT) measured the force required to drive a flat-tip alumina penetrator ($\Phi = 2.8$ mm, $L = 360$ mm) into the specimen. The load data were recorded via an analog–digital converter (Omega D1521, Stamford, CT). A variable speed motor coupled through a variable gear reduction system drove the penetrator at speeds of from 6.4 to 64 mm/h.

2.2. Specimen preparation

Type 1 OPC (Holnam Cement, Clarksville, MO) and ASTM C 778 graded silica sand (AGSCO, IL) were used. Materials were mixed with deionized water using a paddle mixer (Kitchenaid, Model K5SS) for 10 min at speed level 1. The w/c ratio of mortar was fixed at 0.4. Paste or mortar was cast into a polyethylene cylinder ($\Phi = 5$ cm, $L = 10$ cm). Testing and microwave application began 30 min after initial water contact. A constant heating rate of 2 °C/min to the desired set temperature was used. The temperature was maintained until the penetration hardness reached at 20 MPa.

2.3. Experimental designs

Two sets of experiments were performed. The first was designed to obtain an estimate of the activation energy of hardening. For this purpose, cement pastes were mixed at three levels of w/c ratio (0.25, 0.3 and 0.4) and cured at temperatures from 25 to 80 °C. During the elevated temperature curing, the penetration test was performed using the procedures described above.

To further explore the hardening rate, a D-optimal experimental set was designed utilizing available software (EDO) [13]. This methodology was used to reduce the number of experiments needed to describe the response within the chosen parameter space. The three-factor, three-level design was based upon first- and second-order terms and all two-factor multiplicative interactions between the variables. The experimental results were analyzed using multiple regression software (MC) [14] to establish descriptive models for the hardening rate.

Table 1
D-optimal designs for studying hardening rate of cement paste and mortar

	Cement paste			Cement mortar (w/c = 0.4)		
No.	w/c	$1000/T$ (K^{-1})	Gear ratio	s/c	$1000/T$ (K^{-1})	Gear ratio
1	0.4	3.00	100	2	3.00	100
2	0.4	3.30	100	2	3.00	10
3	0.3	3.30	100	2	3.30	100
4	0.3	3.00	100	0	3.00	100
5	0.35	3.30	50	2	3.14	50
6	0.4	3.00	10	1	3.00	50
7	0.35	3.14	100	1	3.14	100
8	0.4	3.30	50	0	3.14	10
9	0.4	3.14	10	0	3.30	50
10	0.3	3.14	10	0	3.00	10
11	0.3	3.00	10	1	3.14	10
12	0.3	3.14	50	0	3.30	100

Table 1 shows the D-optimal designs for cement paste (variables: w/c ratio, inverse temperature and gear ratio) and cement mortar [variables: sand/cement (s/c) ratio, inverse temperature and drive gear ratio]. Gear ratios of 10, 50 and 100 resulted in speeds of 64, 12.8 and 6.4 mm/h, respectively. To facilitate analysis, the levels of each of the independent variables were coded over the range -1 (minimum) to 1 (maximum). Temperature was coded as the reciprocal of the absolute temperature.

3. Results and discussion

3.1. Hardening rate

For this study, the penetration hardness is defined as follows (Eq. (1)):

$$\text{Penetration hardness } (H) = \text{Force}/\text{Frontal area of penetrator} \quad (1)$$

It was found that any frictional effect between penetrator and specimen during testing can be ignored [10,11]. The penetrator could be withdrawn from the specimen after final set without significant frictional drag, indicating that the hole punched in the material by the penetrator tip was slightly larger than the penetrator.

Fig. 2 shows the penetration hardness development for cement pastes (w/c = 0.3) at various temperatures. The beginning of the increase in penetration hardness may closely correspond to the beginning of the acceleration period in the cement–water reaction. Higher curing temperatures are associated with shorter starting times and faster hardness development.

The slightly curved lines in Fig. 2 are represented well as second-order functions of time as follows (Eq. (2)):

$$\ln H = A + Bt + Ct^2$$

(t = time after mixing; A, B and C = constants.) (2)

Then, the hardening rate can be computed from these equations using (Eq. (3)):

$$dH/dt = (d\ln H/dt)\ H \quad (3)$$

Hardening rates were determined at four levels of hardness (1, 5, 9 and 13 MPa) for each penetration test in the D-

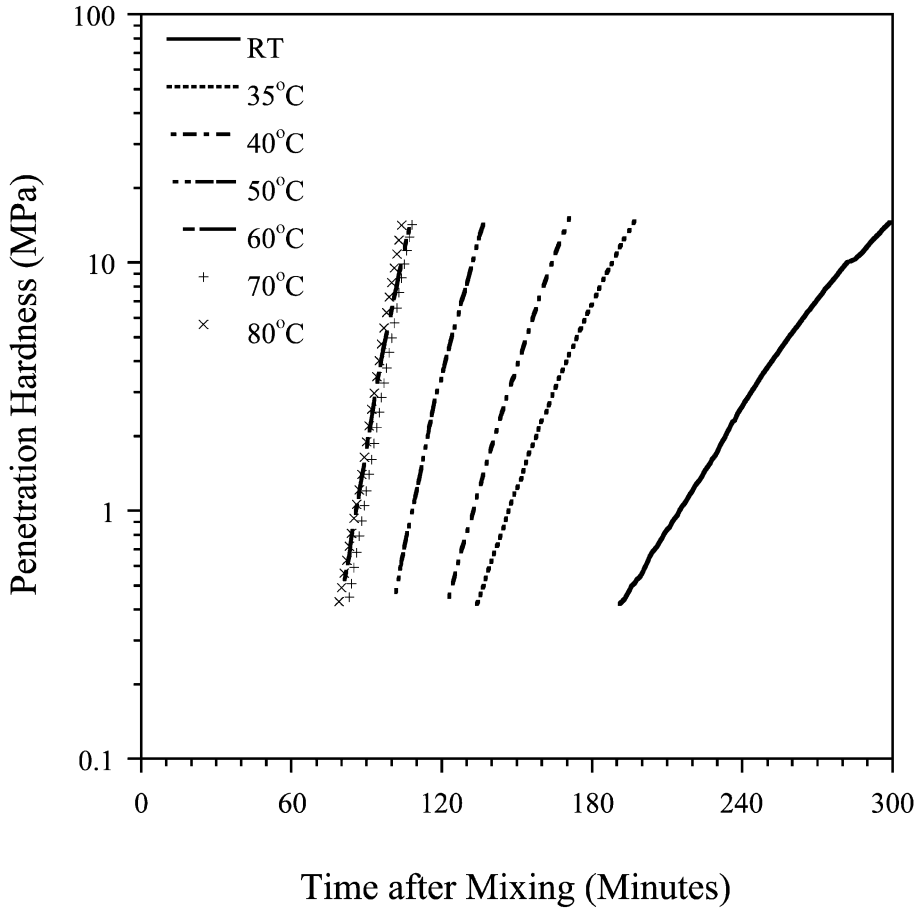

Fig. 2. Semilog plot of penetration hardness for cement paste (w/c = 0.3).

optimal set. This provided a fourth variable and a total of 48 data points for analyzing the hardening rate response surface for each material.

If the microstructure (or degree of hydration) at a given degree of hardness is independent of temperature, the apparent activation energy can be estimated from the hardening rate data. Arbitrarily choosing 5 MPa for H for the first set of experiments, the hardening rates at various w/c ratios and curing temperatures were determined. The data are shown on an Arrhenius plot in Fig. 3(a). Below 60 °C (Region 1), the hardening rates at all w/c are approximately linearly dependent upon reciprocal temperature. However, above 60 °C (Region 2), the hardening rates deviate from the line made in Region 1 to converge to a single point at 80 °C. This temperature dependent behavior was also found in the activation energy of fine β-C_2S [15]. It is thought to be caused by a change in reaction chemistry in the higher temperature range. Specifically, ettringite cannot be formed at 80 °C [16]. The estimated activation energy of the hardening rate in the 25–60° range varied from 26.8 to 35.2 KJ/mol, depending upon the water content. The reported value of activation energies for C_3S and β-C_2S hydration are 31.4 [17] and 57 kJ/mol [15], respectively.

However, estimating the activation energy by the assumption that the rate of hardening is linearly dependent

Table 2
Coefficients of the ln (hardening rate) response surface equations for cement pastes and mortars

	Cement paste: r^2=.998, df=36		Cement mortar: r^2=.993, df=38	
Variable	Coefficient	t value	Coefficient	t value
Intercept	−0.725	–	−0.733	–
Hardness (H)	0.670	19.1	0.682	12.8
w/c ratio (W)	−0.082	−9.7	–	–
s/c (S)	–	–	−0.026	−1.9
1000/T (T)	−0.526	−48.2	−0.603	−39.6
Gear ratio (R)	−0.118	−12.5	−0.094	−6.5
H^2	−0.631	−38.1	−0.635	−25.3
H^3	0.411	11.1	0.411	7.3
T^2	−0.132	−7.9	−0.122	−4.8
R^2	0.140	−6.9	–	–
HR	−0.073	−6.4	−0.084	−4.8
HW	0.039	3.6	–	–
WT	−0.048	−4.7	–	–
SR	–	–	0.045	3.0

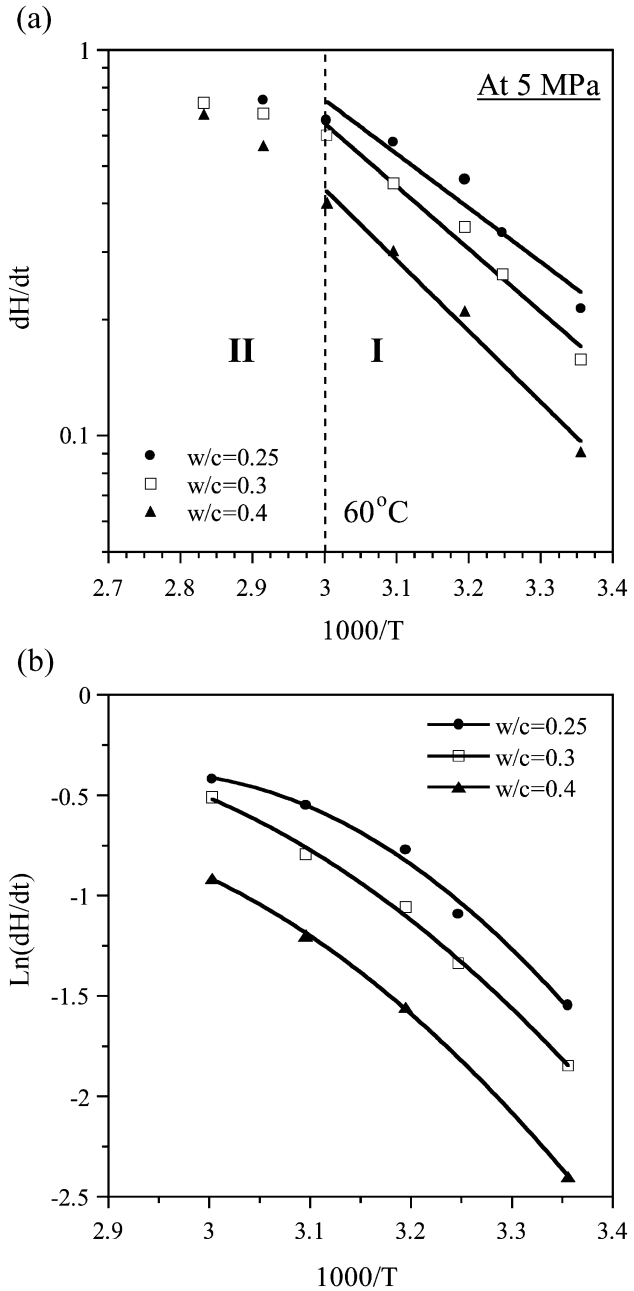

Fig. 3. (a) Arrhenius plot of the rate of hardening at 5 MPa of the penetration hardness for cement pastes with various w/c ratio cured by microwaves. (b) Second-order polynomial curve fitting from 25 °C to 60 °C.

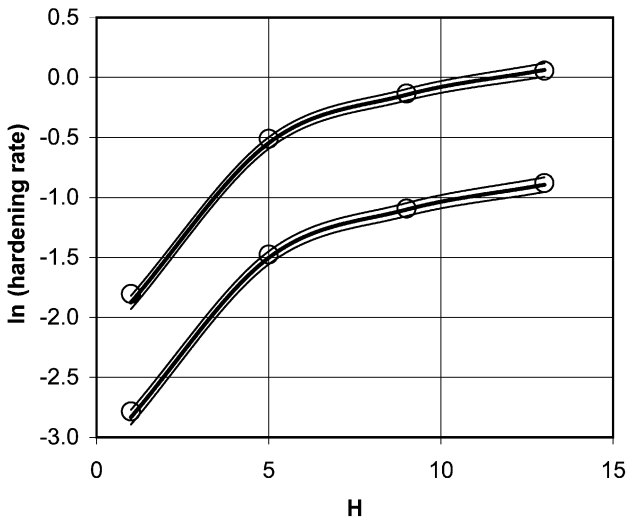

Fig. 4. Model response curves for paste at 30° (lower) and 60 °C (upper) together with 95% confidence intervals. Penetration rate = 6.4 mm/h and w/c = 0.3. Circles are experimental data points.

on inverse temperature is somewhat risky, because the hardening rate may not be a simple function of temperature. Fig. 3(b) shows that a second-order polynomial fits the $< 60^\circ$ portion of the Arrhenius plot better than a straight line. Possible reasons for the complicated temperature dependence may be the multiplicity of cement hydration reactions and possible temperature effects on rheology. The temperature effects on cement rheology have been explored and will be discussed elsewhere [18].

The response surface coefficients and their corresponding t values for ln(hardening rate) resulting from MC analysis are listed in Table 2. (Note: The t value for a coefficient is the ratio of the coefficient to its standard deviation and is a measure of the significance of the variable.) The coefficients are for coded independent variables (from -1 to 1).

3.2. Cement paste

Fig. 4 shows the comparison of actual data and the predicted lines. The solid lines in the figure represent the predicted values of ln(hardening rate) at w/c = 0.3 and penetration rate = 6.4 mm/h and the 95% confidence bands. The good fit shown in this figure, the high value of r^2 and the large number of degrees of freedom (see Table 2) indicate that the equations adequately describe the response. As expected, high temperature enhances the rate of hardening. The hardening rate clearly does not follow Arrhenius behavior since there is a second-order term in reciprocal temperature in the equations. High water amounts make the material softer and also reduce the hardening rate.

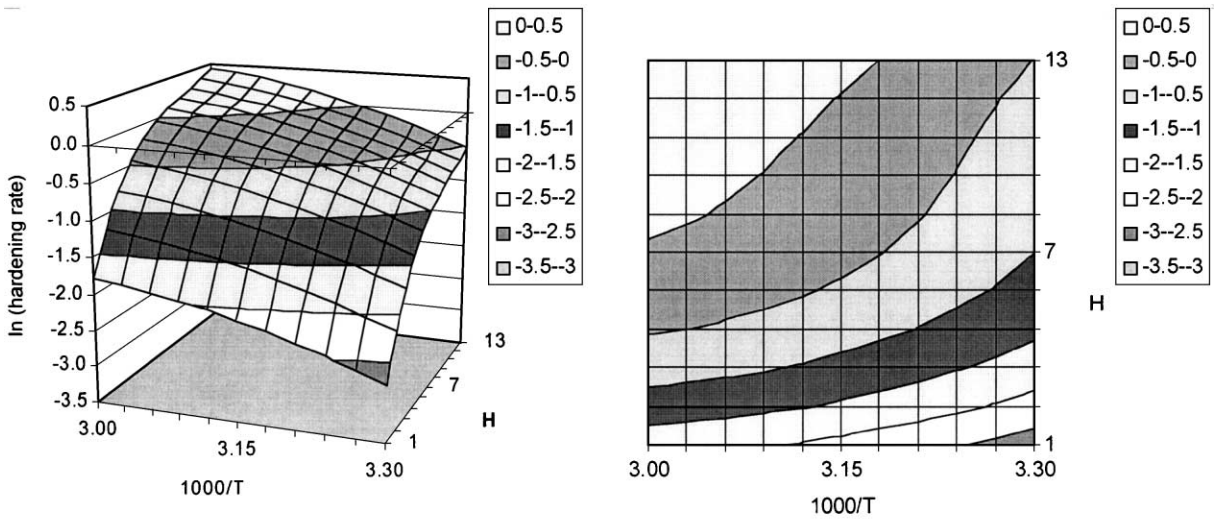

(a) w/c = 0.3; penetration rate = 64 mm/hr

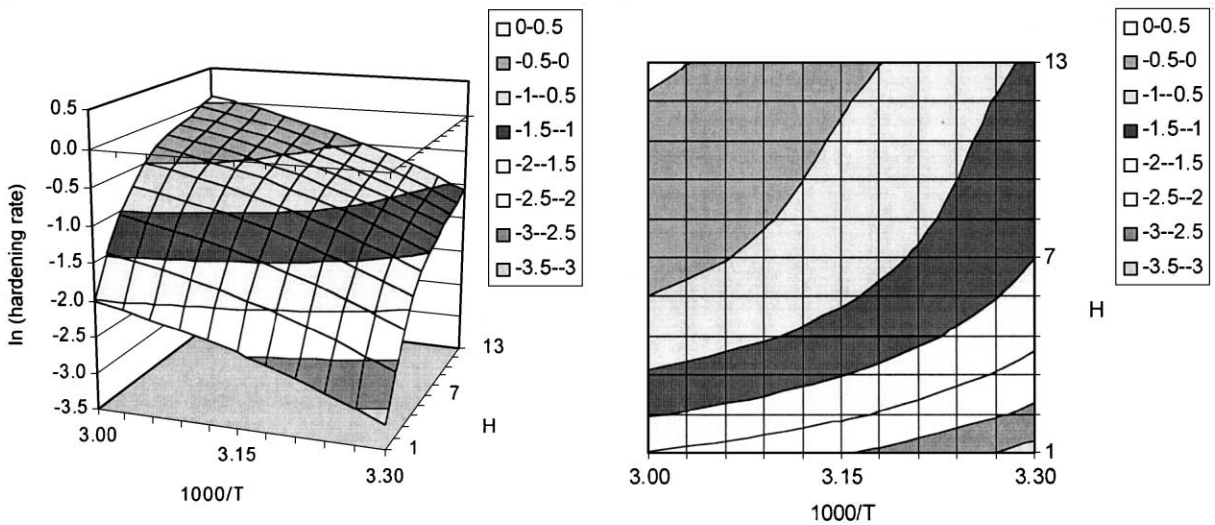

(b) w/c = 0.4; penetration rate = 6.4 mm/hr

Fig. 5. ln (hardening rate) response surface and contour plot for cement paste.

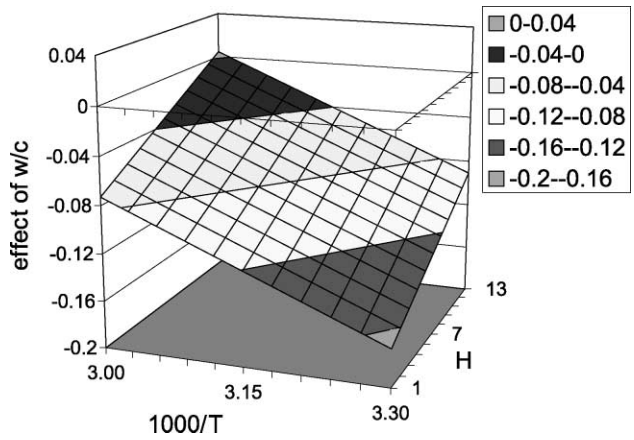

Fig. 6. Effect of the water to cement ratio on the rate of hardening of paste (see Eq. (5)).

The non-Arrhenius behavior indicates that the measured penetration hardness may be a function of the rheology of the paste. If the penetration hardness is a function only of the degree of hydration, then Arrhenius behavior is expected. If the viscosity decreases with increasing temperature at constant degree of hydration, then curvature similar to that shown in Fig. 3(b) would be expected.

It can be seen in Table 2 that of the variables tested, temperature and hardness have the greatest effect on the hardening rate. Fig. 5 shows ln(hardening rate) response surfaces and contour plots of cement pastes as a function of these variables under the extreme cases of low w/s and high penetration rate (tending to high hardening rate) and high w/s and low penetration rate (tending to low hardening rate).

Table 2 also shows three interactions between pairs of variables for cement paste (HR, HW and WT). An interaction exists if the effect of one variable depends upon the level of another. Thus, for example, the effect of hardness H on the hardening rate depends upon the value of the penetration rate represented by R.

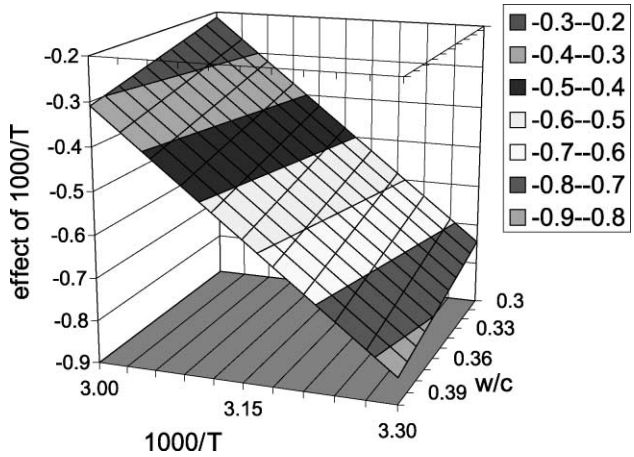

Fig. 7. Effect of $1000/T$ on the rate of hardening of paste (see Eq. (6)).

The effects of the variables and the interaction terms can be explored by partial differentiation of the hardening rate equation with respect to each of the independent variables. Note that all independent variables in Eqs. (4)–(7) are coded from -1 to 1.

$$\text{Hardness}: \quad \frac{\partial(\ln(\mathrm{d}H/\mathrm{d}t))}{\partial(H)} = 0.67 - 1.26(H) + 1.23(H^2) + 0.039(\mathrm{w/c}) - 0.073(R) \tag{4}$$

$$\text{w/c ratio}: \quad \frac{\partial(\ln(\mathrm{d}H/\mathrm{d}t))}{\partial(\mathrm{w/c})} = -0.082 + 0.039(H) - 0.048(1000/T) \tag{5}$$

$$1000/T: \quad \frac{\partial(\ln(\mathrm{d}H/\mathrm{d}t))}{\partial(1000/T)} = -0.53 - 0.26(1000/T) - 0.048(\mathrm{w/c}) \tag{6}$$

$$R: \quad \frac{\partial(\ln(\mathrm{d}H/\mathrm{d}t))}{\partial(R)} = -0.12 + 0.28R - 0.073H \tag{7}$$

The essence of these equations is captured in Figs. 6–8, which are plots of Eqs. (5)–(7), respectively. Fig. 6 shows that the effect of increasing w/c is to reduce the hardening rate over almost all of the temperature–hardness parameter space. The effect is particularly strong at low temperature and low hardness and diminishes to nearly no effect at all as the temperature and hardness increase to their maximum values. In Fig. 7, we observe that raising the temperature (lowering $1000/T$) increases the rate of hardening, but the effect is less at lower w/c ratios.

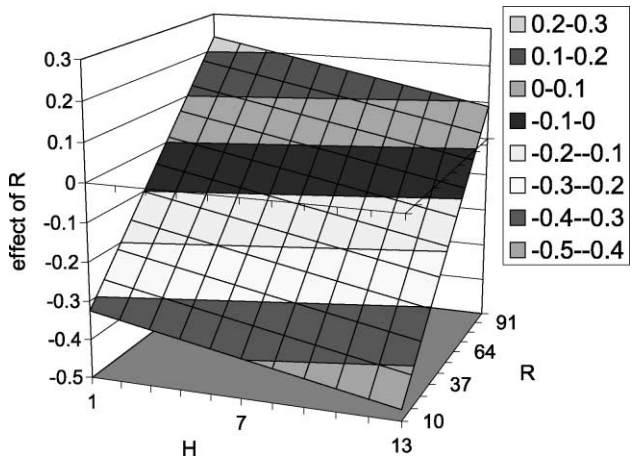

Fig. 8. Effect of gear ratio (reciprocal of penetration rate) on the hardening rate of paste (see Eq. (7)).

Decreasing R (increasing the penetration rate) decreases the hardening rate over much of the parameter space, but the tendency is reversed at low hardness and low penetration rates (high R; Fig. 8). Changing the penetration rate is not expected to change the hydration process but it has significance on the hardening rate because of the nature of the penetration test. It already has been seen that the hardening rate is non-Arrhenius, indicating a possible rheological component to the response. The dependence of the hardening rate on the penetration rate further substantiates this.

3.3. Cement mortar

The equations in Table 2 indicate that the hardening process of cement mortar is very similar to cement paste because the signs of the major factors, such as hardness, temperature and penetration rate, are exactly the same as those shown in the paste equation. The magnitudes also are comparable. The hardness–penetration rate interaction also exists with the same sign and magnitude. Obviously, the terms involving the w/c ratio are missing since this was not varied. The s/c ratio affects the equation in the first order and an interaction with penetration rate, but its level of importance is small. As expected in the equation, the response surface for cement mortar is similar to that of cement paste (Fig. 5). Thus, inert silica sand contributes little to the hardening process of early cement hydration and acts only as a filler. However, if reactive sand is used, sand may influence the hardening process.

The effect of the s/c ratio–gear ratio interaction can be estimated by partial differentiation, as follows:

$$\text{s/c ratio}: \quad \frac{\partial(\ln(\mathrm{d}H/\mathrm{d}t))}{\partial(\mathrm{s/c})} = -0.026 + 0.045(R) \qquad (8)$$

From Eq. (8), we see that increasing the s/c ratio reduces the hardening rate at high penetration rate ($R=-1$) while increases the hardening rate a small amount at the slowest penetration rate ($R=1$). The presence of the s/c ratio–gear ratio interaction implies that the sand content may influence penetration hardness rheologically rather than chemically.

4. Conclusions

The instrumented penetration test provides useful information about the early hardening process for cement-based materials. Microwave heating enhances curing of cement paste and mortar significantly. D-optimal experimental design and multiple regression analysis revealed that the most significant factors in the hardening rate models for mortar as well as cement paste are hardness level, temperature and w/c ratio. Generally, raising the temperature or reducing the water content makes the hardening rate greater. Adding inert silica sand influences the hardening rate rheologically rather than chemically.

Acknowledgments

This work was supported by the National Science Foundation through the Science and Technology Center for Advanced Cement-Based Materials under grant no. CHE-91-20002. Multiple Correlation (MC) and Experimental Design Optimizer (EDO) software courtesy Harold H. Haller & Co., Cleveland, OH. Microwave system courtesy of E. Khoshoggi Industries, Santa Barbara, CA.

References

[1] T.C. Powers, The Properties of Fresh Concrete, Wiley, New York, NY, 1968.
[2] I. Soroka, Portland Cement Paste and Concrete, Macmillan Press, London, UK, 1979.
[3] S. Mindess, J.F. Young, Concrete, Prentice-Hall, Englewood Cliffs, NJ, 1981.
[4] P.K. Mehta, P.J.M. Monteiro, Concrete: Structure, Properties, and Materials, second ed., Prentice-Hall, Englewood Cliffs, NJ, 1993.
[5] A.M. Neville, Properties of Concrete, Wiley, New York, NY, 1996.
[6] A. Bilodeau, V.M. Malhotra, Concrete incorporating high volumes of ASTM class F ashes: Mechanical properties and resistance to deicing salt scaling and to chloride penetration, Proceedings, 4th International Conference on Fly Ash, Silica Fume, Slag and Natural Pozzolans in Concrete, ACI SP 132, Detroit, MI, vol. 1, 1992, pp. 319–350.
[7] O. Eren, J.J. Brooks, T. Celik, Setting times of fly ash and slag–cement concretes as affected by curing temperatures, Cem., Concr., Aggregates 17 (1) (1995) 11–17.
[8] S.H. Gebler, P. Klieger, Effects of fly ash on physical properties of concrete, Proceedings, 2nd International Conference on Fly Ash, Silica Fume, Slag and Natural Pozzolans in Concrete, ACI SP 91, Detroit, MI, vol. 1, 1986, pp. 1–50.
[9] V.S. Ramachandran, R.F. Feldman, J.J. Beaudoin, Concrete Science, Heyden & Son, Philadelphia, PA, 1981.
[10] B.A. Croft, In situ strength development of microwave cured ordinary Portland cement pastes, MS Thesis, Northwestern University, Evanston, IL, 1996.
[11] B.A. Croft, D.L. Johnson, Continuous monitoring of microwave curing of Portland cement, unpublished, 1999.
[12] D. Sohn, D.L. Johnson, unpublished, 1999.
[13] Harold S. Haller & Company, Experimental Design Optimizer, Harold S. Haller & Company, Cleveland, OH, 1992.
[14] Harold S. Haller & Company, Multiple Correlation, Harold S. Haller & Company, Cleveland, OH, 1992.
[15] H. Ishida, K. Sasaki, Y. Okada, T. Mitsuda, Highly reactive β-dicalcium silicate: III, Hydration behavior at 40–80 °C, J. Am. Ceram. Soc. 75 (9) (1992) 2541–2546.
[16] D.F. Orchard, A.M. Barnett, The electrocuring of concrete test specimens, J. Mater., JMLSA 6 (1971) 617–642.
[17] K. Fujii, W. Kondo, Kinetics of the hydration of tricalcium silicate, J. Am. Ceram. Soc. 57 (11) (1974) 492–497.
[18] D. Sohn, D.L. Johnson, unpublished, 1999.